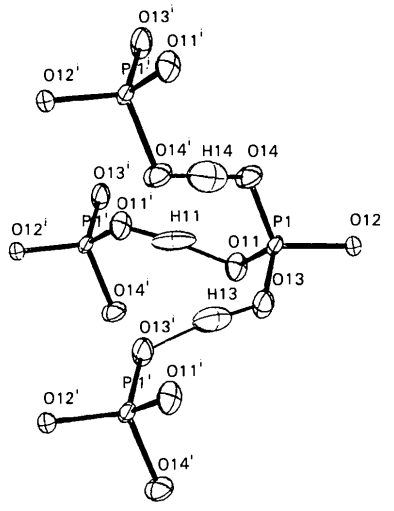

Fig. 2. The three hydrogen bonds that cross pseudo centers of symmetry. O(14)—H(14)—O(14^{i}) is still nearly symmetric in $P\bar{1}$. All of the hydrogen atoms have large amplitudes of thermal motion parallel to the bond.

Fig. 2 shows the three hydrogen bonds involving the hydrogen atoms that occupy centers of symmetry in models 1 and 2. It is apparent that all three of these hydrogen atoms have large amplitudes of thermal vibration nearly parallel to the O—O vector, which implies that the potential wells, whether they have single or double minima, are rather flat in that direction.

This investigation was supported in part by Research Grant DE 05030-05 to the American Dental Association Health Foundation by the National Institute of Dental Research and is part of the Dental Research Program conducted by the National Bureau of Standards in cooperation with the American Dental Association Health Foundation.

References

BROYDEN, C. G. (1972). *Numerical Methods for Unconstrained Optimization*, edited by W. MURRAY, pp. 87–106. London and New York: Academic Press.

FINGER, L. W. & PRINCE, E. (1975). *Natl Bur. Stand (US) Tech. Note* No. 854. National Bureau of Standards, Washington, DC.

FLATT, R., BRUNISHOLZ, G. & CHAPUIS-GOTTREUX, S. (1951). *Helv. Chim. Acta*, **34**, 884–894.

HAMILTON, W. C. (1959). *Acta Cryst.* **12**, 609–610.

HAMILTON, W. C. (1965). *Acta Cryst.* **18**, 502–510.

International Tables for X-ray Crystallography (1974). Vol. IV, pp. 99–102. Birmingham: Kynoch Press.

JOHNSON, C. K. (1965). *ORTEP*. Report ORNL-3794. Oak Ridge National Laboratory, Tennessee.

LENHERT, P. G. (1975). *J. Appl. Cryst.* **8**, 568–570.

NICHOLSON, W. L., PRINCE, E., BUCHANAN, J. & TUCKER, P. (1983). *Crystallographic Statistics, Progress and Problems*, edited by S. RAMASESHAN, M. F. RICHARDSON & A. J. C. WILSON, pp. 229–263. Bangalore: Indian Academy of Sciences.

PRINCE, E. (1972). *J. Chem. Phys.* **56**, 4352–4355.

STEWART, J. M., MACHIN, P. A., DICKINSON, C. W., AMMON, H. L., HECK, H. & FLACK, H. (1976). *XRAY76*. Tech. Rep. TR446. Computer Science Center, Univ. of Maryland, College Park, Maryland.

TAKAGI, S., MATHEW, M. & BROWN, W. E. (1980). *Acta Cryst.* B**36**, 766–771.

ZACHARIASEN, W. H. (1967). *Acta Cryst.* **23**, 558–564.

Acta Cryst. (1984). C**40**, 1502–1506

Trithallium Tetraselenophosphate, Tl_3PSe_4, and Trithallium Tetrathioarsenate, Tl_3AsS_4, by Neutron Time-of-Flight Diffraction

BY R. W. ALKIRE, PHILLIP J. VERGAMINI AND ALLEN C. LARSON

Los Alamos National Laboratory, Los Alamos, New Mexico 87545, *USA*

AND BRUNO MOROSIN

Sandia National Laboratories, Albuquerque, New Mexico 87185, *USA*

(*Received* 2 *September* 1983; *accepted* 25 *April* 1984)

Abstract. Room-temperature (293 K) single-crystal structure determinations of the isostructural materials Tl_3PSe_4 and Tl_3AsS_4 were performed at the Los Alamos National Laboratory Pulsed Neutron Facility. For Tl_3PSe_4: $M_r = 959{\cdot}92$, *Pcmn*, $a = 9{\cdot}276$ (1), $b = 11{\cdot}036$ (2), $c = 9{\cdot}058$ (1) Å, $V = 927{\cdot}27$ Å^3, $Z = 4$, $D_m = 6{\cdot}87$ (2), $D_x = 6{\cdot}876$ Mg m^{-3}, $\lambda_{neutron} = 0{\cdot}5 \rightarrow 5{\cdot}2$ Å, $F(000) = 252{\cdot}5$ fm. For Tl_3AsS_4: $M_r = 816{\cdot}29$, *Pcmn*, $a = 9{\cdot}084$ (3), $b = 10{\cdot}877$ (3), $c = 8{\cdot}877$ (3) Å, $V = 877{\cdot}11$ Å^3, $Z = 4$, $D_m = 6{\cdot}18$ (2), $D_x = 6{\cdot}181$ Mg m^{-3}, $\lambda_{neutron} = 0{\cdot}5 \rightarrow 5{\cdot}2$ Å, $F(000) = 177{\cdot}2$ fm. For Tl_3PSe_4 (Tl_3AsS_4), 1929 (1013) reflections were measured with $I > 3\sigma(I)$ and refined by full-matrix least squares to $R(F) = 0{\cdot}061$ (0·063). Results on atomic refinement from this study represent an order of magnitude increase in precision over

0108-2701/84/091502-05$01.50

previous single-crystal X-ray structural work using Mo $K\alpha$ radiation. The PSe_4^{3-} (AsS_4^{3-}) groups have essentially tetrahedral configurations and one Tl^+ ion shows large anisotropic thermal motion which is structure related.

Introduction. Tl_3PSe_4 and Tl_3AsS_4 are two members of a large family of chalcogenide crystals (Tl_3AsSe_3, Tl_3VS_4, $TlGaSe_2$, $AgAsS_3$ and others) which have potential applications in acousto-optic devices. Such devices include optical filters, laser modulators, deflectors and signal processors, to name a few. These isostructural materials are particularly important because their optical transmission is quite high (60–90% in the 0·8 – 8 μm region) and their acoustic (shear-wave) velocities are among the lowest of any solid or liquid recorded in the literature, apart from those velocities associated with critical-point phenomena. Low acoustic-wave velocities also make these materials potentially useful for miniature delay lines. For example, by using the slow shear mode in Tl_3PSe_4 ($1{\cdot}2 \times 10^5$ cm s^{-1} [001] propagation direction) it is possible to produce a 10 μs delay using a crystal that is only 5 mm long (Gottlieb, Isaacs, Feichtner & Roland, 1974).

Interest in these materials has also been generated by the discovery of pressure-induced structural phase transitions with related softening of the anomalous shear mode. These transitions were confirmed for Tl_3PSe_4 (Fritz, Isaacs, Gottlieb & Morosin, 1978) and Tl_3AsS_4 (Fritz, Gottlieb, Isaacs & Morosin, 1981) using ultrasonic (pulse echo) techniques and appear to be completely reversible. Measurements on Tl_3PSe_4 as a function of temperature also show a linear decrease in the *ab* shear mode velocity, but no temperature-induced structural phase transition has been observed (Fritz *et al.*, 1978).

Atomic positions were originally determined for these compounds using Mo $K\alpha$ radiation (Fritz *et al.*, 1978). These compounds are relatively soft, however, and morphology of the single-crystal specimens used was ill defined. Consequently, correcting measured intensities for absorption proved difficult [*e.g.* μ(Mo $K\alpha$) = 1250 cm^{-1} for Tl_3AsS_4] and led to rather high standard deviations on the atomic positions. In order to reduce uncertainties in atomic positions as well as obtain meaningful thermal parameters which might offer insight into the incipient lattice instability associated with ultrasonic measurements, both structures were redetermined using single-crystal neutron diffraction data.

Time-of-flight diffraction

Single-crystal neutron diffraction using the time-of-flight technique was explored as early as 1965 (Buras, Mikke, Lebech & Leciejewicz, 1965) on a steady-state reactor. With the advent of pulsed neutron sources (Peterson, Reis, Schultz & Day, 1980; Carpenter, 1977) much effort has been devoted to developing the time-of-flight technique for routine single-crystal structure analysis (Day, Johnson & Sinclair, 1969; Lebech, Mikke & Sledziewska-Blocka, 1970; Day & Sinclair, 1970; Niimura, Kubota, Sato, Arai & Ishikawa, 1980; Schultz, Teller, Peterson & Williams, 1982; Larson & Vergamini, 1981). Recent advances at Los Alamos National Laboratory (Larson & Vergamini, 1982) and elsewhere (Schultz, Teller, Beno, Williams, Brookhart, Lamanna & Humphrey, 1983) have refined the technique so that routine crystal structure analysis is now possible.

The time-of-flight technique is considerably different from conventional diffraction techniques in that the Laue method is used for measuring Bragg diffracted intensities. Here, the crystal is stationary and the detector is set at a fixed 2θ angle. According to Bragg's Law ($n\lambda = 2d\sin\theta$), all orders (n) of a Bragg plane diffract energy at wavelengths λ_1/n (λ_1 is the first order) and each of these orders hits the same spot on the detector. Obvious difficulties are encountered if polychromatic X-rays are used in the experiment since all diffraction maxima from a single Bragg plane occur simultaneously on the detector (commonly one spot on a film). Discrete wavelength information is lost and, therefore, so is the ability to separate individual *hkl* intensities. With pulsed neutron sources wavelength information is retained. Polychromatic neutrons produced in a single burst leave the target moderator and, due to differences in their velocities, are separated by time-of-flight over a fixed moderator to detector distance. Quantitative integrated intensities can be measured, then, because each solution (λ_1/n) to the Bragg equation arrives at the detector separated in time.

In addition to collecting multi-wavelength data, enhanced data-collection rates can be achieved by utilizing a two-dimensional (spatial) area detector; this allows a large section of reciprocal space to be examined with a single, fixed setting of the crystal. Each such setting (histogram) measures all the diffracted intensity as well as systematic absences in a particular volume of reciprocal space (defined by the wavelength range, crystal orientation, and instrument parameters). Depending on the instrument settings, a full set of data for an orthorhombic crystal (including some overlap of adjacent histograms to ensure complete coverage of all unique data) can typically be measured with twelve crystal settings.

Experimental. Single crystals of Tl_3PSe_4 (Tl_3AsS_4) $2{\cdot}96 \times 2{\cdot}86 \times 2{\cdot}86$ mm ($2{\cdot}90 \times 2{\cdot}80 \times 2{\cdot}60$ mm) mounted on a GE quarter circle* with a detection

* The single-crystal diffractometer at LANL has been redesigned since completion of this work and will support low-temperature capabilities. Specialized apparatus is also being designed for high-pressure and high-temperature work.

system consisting of a Borkowski–Kopp-type position-sensitive proportional counter (Borkowski & Kopp, 1978) filled with 2×10^5 Pa of $^3He + Xe + CO_2$. Detector center (active area 25 × 25 cm) was located 90° to the incident beam and 26 cm from the crystal; crystal to moderator distance was 578 cm. Each event on the detector was encoded within a framework consisting of 64 × 64 spatial (or x,y) channels and a time resolution of 128 channels covering the wavelength range 0·5→5·2 Å. Time channels were divided into nearly equal increments of $1/d$ and individual x,y channels were equally spaced across the detector.

Initial lattice parameters were taken from the X-ray structure and further refined using peak intensities from 100 reflections measured in the range 66→114° (2θ). Space group *Pcmn* (*cba* setting of *Pnma*; general positions $\pm x,y,z$; $\pm\frac{1}{2}-x,y,\frac{1}{2}+z$; $\pm x,\frac{1}{2}-y,z$; $\pm\frac{1}{2}-x,\frac{1}{2}-y,\frac{1}{2}+z$) has been retained for these structures to remain consistent with earlier X-ray work as well as with rules suggested by Kennard, Speakman & Donnay (1967); neutron transmission values range from 0·87 to 0·75 (0·94 to 0·89). Densities were measured by Berman torsion balance.

Conversion of integrated intensities to structure factor amplitudes is based on the Laue formula (Buras *et al.*, 1965; Schultz *et al.*, 1982)

$$I_{hkl} = kT\varphi(\lambda)\varepsilon(\lambda)A(\lambda)y|F_{hkl}|^2\lambda^4/\sin^2\theta,$$

where k is the scale factor, T the normalized monitor count, F_{hkl} the structure factor, θ the Bragg angle, $\varphi(\lambda)$ the incident neutron flux, $\varepsilon(\lambda)$ the detector efficiency, $A(\lambda)$ the absorption correction for wavelength λ, and y the extinction correction. $\varphi(\lambda)$ and $\varepsilon(\lambda)$ were obtained as a single normalization factor from incoherent scattering off a 3 mm diameter vanadium bead (Lebech *et al.*, 1970; Day *et al.*, 1969); the vanadium bead is doped with 5·5 at. % niobium to form a composite null coherent scatterer. Absence of neutron resonances (Mughabghab & Garber, 1973; Garber & Kinsey, 1976) in the 0·5→5·2 Å wavelength range for Tl, P, Se, As and S allows linear absorption coefficients to be calculated as follows: Tl_3PSe_4: $\mu(cm^{-1}) = 0{\cdot}286 + 0{\cdot}069\lambda$; Tl_3AsS_4: $\mu(cm^{-1}) = 0{\cdot}179 + 0{\cdot}021\lambda$.

Approximately two independent units of data were collected for Tl_3PSe_4 covering $h = \pm 15$, $k = -3, 19$, $l = -3, 15$ with 3213 reflections measured, 1929 observed [$I > 3\sigma(I)$]; approximately one independent unit was measured on Tl_3AsS_4, $h = -14, 2$, $k = -19, 2$, $l = -14, 2$ with 1746 reflections measured, 1013 observed [$I > 3\sigma(I)$]; max. $\sin\theta/\lambda$ used in the least-squares refinement was 1·00 (1·00) Å^{-1}. Due to the variation of extinction and absorption with wavelength in time-of-flight diffraction, all measured reflections were treated as independent observations, *i.e.* 'equivalent' reflections were not averaged. Data reduction and least-squares refinement were performed using the Los Alamos crystal structure programs (Larson, 1977). Refinements of both structures were carried out using anisotropic temperature factors and an isotropic extinction parameter. The extinction correction y_i is based on the formula (Becker & Coppens, 1974*a*,*b*)

$$y_i = \left[1 + 2x_i + \frac{A(\theta)x_i^2}{1 + B(\theta)x_i}\right]^{-1/2},$$

where $A(\theta)$ and $B(\theta)$ are angular dependent coefficients and x_i the extinction parameter for i = primary or secondary extinction; definition of x_i depends on the extinction model chosen, *i.e.* type I, type II, or a combination of types I and II (Zachariasen, 1967). For type I,

$$x_i = k^2\gamma\bar{T}(F_c)^2 g\frac{\lambda^2}{\sin^2\theta},$$

where the symbols are identical to those defined by Becker & Coppens (1974*a*).

Initial positional parameters taken from the previous X-ray study and final least-squares refinement cycles yielded $R(F) = 0{\cdot}061$ (0·063), $wR(F) = 0{\cdot}057$ (0·060), $S = 2{\cdot}41$ (2·31) with $w = [1/\sigma(F_o)]^2$; $(\Delta/\sigma)_{max}$ in the final refinement cycle was 2×10^{-4} (4×10^{-4}); residual nuclear scattering density appearing in the final difference Fourier synthesis was virtually featureless; secondary-extinction modeling of type I yielded a Gaussian half-width of 1·2° for Tl_3PSe_4 and 0·8° for Tl_3AsS_4; nuclear scattering lengths (fm) used in this study: Tl = 8·8, P = 5·1, Se = 8·0, As = 6·6, S = 2·8 (Koester & Yelon, 1982).

Discussion. Table 1 lists refined positional and thermal parameters for Tl_3PSe_4 and Tl_3AsS_4.† Thermal motion of the atoms is defined as $\exp[-2\pi^2(h^2a^{*2}u_{11} + k^2b^{*2}u_{22} + l^2c^{*2}u_{33} + 2hka^*b^*u_{12} + 2hla^*c^*u_{13} + 2klb^*c^*u_{23})]$.

The present refinement represents a significant increase in precision for positional parameters in comparison with previous X-ray results. An improvement of at least an order of magnitude has been achieved. Furthermore, precise anisotropic thermal parameters have been obtained. This is a direct result of reduced absorption in the neutron diffraction experiment, *e.g.* $\mu_{X\text{-ray}} = 1154\ cm^{-1}$ and $\mu_{neutron} = 0{\cdot}64_{max}cm^{-1}$ for Tl_3PSe_4. These isostructural materials consist of layers situated about mirror planes normal to the b axis at $y = \frac{1}{4}$ and $\frac{3}{4}$. Describing Tl_3PSe_4, in each formula unit one Tl, the P and two Se atoms of the nearly tetrahedral PSe_4^{3-} group are situated on the mirror plane; the remaining two Tl and two Se atoms are symmetrically disposed about the plane. Fig. 1

† Lists of structure factors have been deposited with the British Library Lending Division as Supplementary Publication No. SUP 39444 (18 pp.). Copies may be obtained through The Executive Secretary, International Union of Crystallography, 5 Abbey Square, Chester CH1 2HU, England.

Table 1. *Positional and thermal* (Å^2) *parameters*

	x	y	z	u_{11}	u_{22}	u_{33}	u_{12}	u_{13}	u_{23}
Tl_3PSe_4									
Tl(1)	0·3055 (1)	0·4519 (1)	0·5565 (1)	0·0345 (5)	0·0270 (5)	0·0350 (6)	−0·0003 (4)	0·0013 (5)	0·0022 (5)
Tl(2)	0·6139 (2)	¼	−0·1143 (2)	0·0302 (8)	0·0723 (13)	0·0263 (8)	0	0·0045 (7)	0
P	0·4727 (2)	¼	0·2811 (2)	0·0134 (10)	0·0197 (11)	0·0149 (10)	0	0·0009 (9)	0
Se(1)	0·2345 (1)	¼	0·3038 (2)	0·0157 (6)	0·0259 (8)	0·0243 (8)	0	0·0021 (6)	0
Se(2)	0·5665 (1)	¼	0·5050 (2)	0·0183 (6)	0·0302 (8)	0·0165 (6)	0	0·0035 (6)	0
Se(3)	0·5363 (1)	0·0865 (1)	0·1594 (1)	0·0315 (6)	0·0281 (6)	0·0250 (5)	0·0088 (4)	0·0030 (5)	−0·0061 (5)
Tl_3AsS_4									
Tl(1)	0·3042 (1)	0·4506 (1)	0·5615 (1)	0·0333 (6)	0·0237 (6)	0·0311 (6)	−0·0024 (6)	−0·0002 (6)	0·0001 (7)
Tl(2)	0·6096 (2)	¼	−0·1161 (2)	0·0277 (8)	0·0658 (16)	0·0236 (8)	0	0·0018 (7)	0
As	0·4740 (2)	¼	0·2799 (2)	0·0130 (8)	0·0167 (11)	0·0104 (8)	0	0·0003 (7)	0
S(1)	0·2350 (5)	¼	0·3049 (5)	0·0120 (18)	0·0265 (26)	0·0219 (20)	0	0·0002 (18)	0
S(2)	0·5683 (5)	¼	0·5024 (5)	0·0174 (19)	0·0261 (29)	0·0159 (19)	0	0·0016 (17)	0
S(3)	0·5360 (4)	0·0862 (4)	0·1564 (4)	0·0292 (16)	0·0226 (20)	0·0238 (17)	0·0082 (17)	0·0021 (15)	−0·0071 (17)

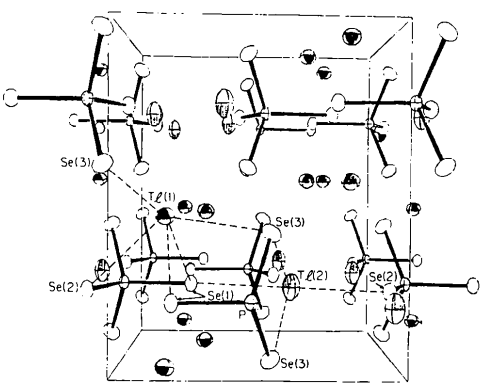

Fig. 1. Tl_3PSe_4 unit-cell packing as viewed along the c axis; dashed lines illustrate the Tl—Se environment within a radius of 3·4 Å.

illustrates this packing arrangement as viewed along the c axis.

Considering Tl—X (X = Se, S) interaction distances within the sum of their ionic radii (Tl—Se 3·38; Tl—S 3·31 Å; *Handbook of Chemistry and Physics,* 1974), Tl(1) has five nearest neighbors (dashed lines in Fig. 1). Closest Tl(1) interactions are those involving $X(1)$, with Tl(1) positioned between the two $X(1)$ atoms at an angle [$X(1)$—Tl(1)—$X(1)$] of ~90°. Remaining Tl(1)—X electrostatic contacts bridge three separate tetrahedral groups and serve as the principal link between layers at $y = \frac{1}{4}$ and $y = \frac{3}{4}$.

For Tl(2), which resides on the mirror plane, four Tl(2)—X nearest neighbors are present; two are in the plane of the mirror and two are symmetrically disposed above and below the mirror forming an angle [$X(3)$—Tl(2)—$X(3)$] of ~70°. Tl(2) exhibits the most unusual feature of these materials in that its anisotropic thermal parameter, u_{22}, is a factor of two greater than any other in the structure. One explanation for this large anisotropic vibration could be a disordering of Tl(2) above and below the mirror. Modeling Tl_3PSe_4 as a disordered structure did show a significant decrease in u_{22} (0·0436 *vs* 0·0723 Å^2) but the distance between disordered Tl(2) positions was only 0·32 Å (equal to one half the square root of the difference) and no improvement in $R(F)$ was obtained as required by such a hypothesis (Hamilton, 1965).

Table 2. *Distances* (Å) *and angles* (°) *for the tetrahedral* PSe_4^{3-} *and* AsS_4^{3-} *groups; nonbonding* Tl(X) *environment*

	PSe_4^{3-}	AsS_4^{3-}
P(As)—$X(1)$*	2·220 (2)	2·183 (5)
P(As)—$X(2)$	2·207 (2)	2·153 (5)
P(As)—$X(3)$	2·196 (2)	2·166 (4)
$X(1)$—P(As)—$X(2)$	107·92 (10)	107·61 (19)
$X(1)$—P(As)—$X(3)$	108·29 (6)	108·06 (12)
$X(2)$—P(As)—$X(3)$	110·83 (6)	111·16 (12)
$X(3)$—P(As)—$X(3')$	110·57 (9)	110·64 (16)
	Tl_3PSe_4	Tl_3AsS_4
Tl(1)—$X(1)$	3·262 (2)	3·217 (4)
Tl(1)—$X(1)$	3·181 (2)	3·091 (4)
Tl(1)—$X(2)$	3·324 (1)	3·285 (4)
Tl(1)—$X(2)$	3·542 (1)	3·502 (2)
Tl(1)—$X(3)$	3·503 (1)	3·443 (4)
Tl(1)—$X(3)$	3·313 (2)	3·250 (4)
Tl(1)—$X(3)$	3·331 (1)	3·228 (4)
Tl(2)—$X(1)$	3·316 (2)	3·207 (5)
Tl(2)—$X(2)$	3·476 (2)	3·407 (5)
Tl(2)—$X(2)$	3·155 (2)	3·110 (5)
Tl(2)—$X(3)$	3·150 (2)	3·077 (4)
Tl(2)—$X(3)$	3·150 (2)	3·077 (4)

* X = Se, S.

A more plausible explanation for the marked anisotropic behavior can be based entirely on steric arguments. Within the plane of the mirror, the nominal $X(1)$—Tl(2)—$X(2)$ angle is 173°. Symmetrically disposed $X(3)$ atoms are located nominally in the bisecting position to the $X(1)$—Tl(2)—$X(2)$ angle. This structural arrangement puts all Tl(2) electrostatic interactions along a line within the plane of the mirror and off to one side perpendicular to the line. Within the distance constraints corresponding to the sum of ionic radii, Tl(2) has no restraining forces opposite $X(3)$ positions. More importantly, $X(3)$ atoms are positioned only 35° above and below the mirror. Without additional electrostatic forces present along the b axis, motion of Tl(2) is restrained only in the plane of the mirror and left relatively free to vibrate perpendicular to the mirror, thus explaining the unusual anisotropic behavior.

Within the precision of our measurement the PSe_4^{3-} (AsS_4^{3-}) groups depart slightly from an idealized tetrahedral arrangement, as indicated by the data in Table 2. The average P—Se bond length is 2·207 Å (As—S 2·167 Å). Individual bond angles are also distorted from perfect tetrahedral geometry, with an average Se—P—Se deviation of 1·5° (S—As—S 1·8°).

Although small geometric distortions exist in the tetrahedral PSe_4^{3-}(AsS_4^{3-}) groups and an unusually large anisotropic thermal parameter exists in these materials, no specific conclusions concerning the observed lattice softening can be drawn at this time. Further structural studies are being conducted on these chalcogenides, including single-crystal neutron structure determinations at 15 K and a high-pressure single crystal neutron structure determination on Tl_3PSe_4 at 1·5 GPa. With room-temperature structure parameters now defined, clearer understanding of the role of structure *versus* solid-state properties (as a function of temperature and pressure) will be possible.

The authors gratefully acknowledge the work of Milton Gottlieb of Westinghouse Research and thank him for supplying the crystals used in this experiment. This work was performed under the auspices of the US Department of Energy, supported in part by Contract DE-AC-0476-DP00789.

References

BECKER, J. P. & COPPENS, P. (1974*a*). *Acta Cryst.* A**30**, 129–147.

BECKER, J. P. & COPPENS, P. (1974*b*). *Acta Cryst.* A**30**, 148–153.

BORKOWSKI, C. J. & KOPP, M. K. (1978). *J. Appl. Cryst.* **11**, 430–434.

BURAS, B., MIKKE, K., LEBECH, B. & LECIEJEWICZ, J. (1965). *Phys. Status Solidi*, **11**, 567–573.

CARPENTER, J. M. (1977). *Nucl. Instrum. Methods*, **145**, 91–113.

DAY, D. H., JOHNSON, D. A. G. & SINCLAIR, R. N. (1969). *Nucl. Instrum. Methods*, **70**, 164–168.

DAY, D. H. & SINCLAIR, R. N. (1970). *Acta Cryst.* B**26**, 2079–2085.

FRITZ, I. J., GOTTLIEB, M., ISAACS, T. J. & MOROSIN, B. (1981). *J. Phys. Chem. Solids*, **42**, 269–273.

FRITZ, I. J., ISAACS, T. J., GOTTLIEB, M. & MOROSIN, B. (1978). *Solid State Commun.* **27**, 535–539.

GARBER, D. I. & KINSEY, R. R. (1976). *Neutron Cross Sections.* BNL 325, 3rd ed., Vol. III. Brookhaven National Laboratory, Upton, NY.

GOTTLIEB, M., ISAACS, T. J., FEICHTNER, J. D. & ROLAND, G. W. (1974). *J. Appl. Phys.* **45**, 5145–5151.

HAMILTON, W. C. (1965). *Acta Cryst.* **18**, 502–510.

Handbook of Chemistry and Physics (1974). Edited by ROBERT C. WEAST, pp. F198-F199. Cleveland, Ohio: CRC Press.

KENNARD, O., SPEAKMAN, J. C. & DONNAY, J. D. H. (1967). *Acta Cryst.* **22**, 445–449.

KOESTER, L. & YELON, W. B. (1982). *Compilation of Low Energy Neutron Scattering Lengths and Cross Sections.* ECN, Netherlands Energy Research Foundation, Department of Physics.

LARSON, A. C. (1977). *Program and Abstracts.* American Crystallographic Association Summer Meeting, East Lansing, Michigan, paper H8, p. 67.

LARSON, A. C. & VERGAMINI, P. J. (1981). *Acta Cryst* A**37**, C290.

LARSON, A. C. & VERGAMINI, P. J. (1982). *Program and Abstracts*, American Crystallographic Association Winter Meeting, Gaithersburg, MD, Vol. 10, p. 34, paper L5.

LEBECH, B., MIKKE, K. & SLEDZIEWSKA-BLOCKA, D. (1970). *Nucl. Instrum. Methods*, **79**, 51–54.

MUGHABGHAB, S. F. & GARBER, D. I. (1973). *Neutron Cross Sections.* BNL 325, 3rd ed., Vol. I. Brookhaven National Laboratory, Upton, NY.

NIIMURA, N., KUBOTA, T., SATO, M., ARAI, M. & ISHIKAWA, Y. (1980). *Nucl. Instrum. Methods*, **173**, 517–523.

PETERSON, S. W., REIS, A. H. JR, SCHULTZ, A. J. & DAY, P. (1980). *Adv. Chem. Ser.* No. 186, pp. 75–91.

SCHULTZ, A. J., TELLER, R. G., BENO, M. A., WILLIAMS, J. M., BROOKHART, M., LAMANNA, W. & HUMPHREY, M. B. (1983). *Science*, **220**, 197–199.

SCHULTZ, A. J., TELLER, R. G., PETERSON, S. W. & WILLIAMS, J. M. (1982). *AIP Conf. Proc.* No. 89, pp. 35–41.

ZACHARIASEN, W. H. (1967). *Acta Cryst.* **23**, 558–564.

Acta Cryst. (1984). C**40**, 1506–1510

The Structures of Onoratoite, $Sb_8O_{11}Cl_2$ and $Sb_8O_{11}Cl_2.6H_2O$

BY S. MENCHETTI, C. SABELLI AND R. TROSTI-FERRONI

CNR, Dipartimento di Scienze della Terra, Via G. LaPira 4, 50121 *Firenze, Italy*

(*Received* 5 *March* 1984; *accepted* 15 *May* 1984)

Abstract. $Sb_8O_{11}Cl_2$ (I): $M_r = 1220·9$, monoclinic, $C2/m$, $a = 19·047$ (35), $b = 4·0530$ (3), $c = 10·318$ (3) Å, $\beta = 110·25$ (4)°, $V = 747$ (1) Å^3, $Z = 2$, $D_x = 5·425$ Mg m^{-3}, Mo $K\bar{\alpha}$, $\lambda = 0·7107$ Å, $\mu = 14·99$ mm^{-1}, $F(000) = 1060$, room temperature, $R = 0·054$ for 828 observed reflections. All the examined crystals are twinned, with (001) as twin plane. $Sb_8O_{11}Cl_2.6H_2O$ (II): $M_r = 1329·0$, orthorhombic, $Immm$, $a = 9·618$ (3), $b = 13·148$ (6), $c = 4·078$ (1) Å, $V = 515·7$ (3) Å^3, $Z = 1$, $D_x = 4·279$ Mg m^{-3}, Mo $K\bar{\alpha}$, $\lambda = 0·7107$ Å, $\mu = 10·75$ mm^{-1}, $F(000) = 590$, room temperature, $R = 0·038$ for 346 observed reflections. Crystals grown from a cold solution. The structures of (I) and (II) exhibit similar features. Both have Sb–O

0108-2701/84/091506-05$01.50